A recent review of mid-wavelength infrared type-II superlattices: carrier localization, device performance, and radiation tolerance

Elizabeth H. Steenbergen,*[a] Gamini Ariyawansa,[b] Charles J. Reyner,[b] Geoffrey D. Jenkins,[a]
Christian P. Morath,[a] Joshua M. Duran,[b] John E. Scheihing,[b] Vincent M. Cowan[a]

[a]Air Force Research Laboratory, Space Vehicles Directorate, Kirtland AFB, NM, USA 87117;
[b]Air Force Research Laboratory, Sensors Directorate, Wright-Patterson AFB, OH, USA 45433

ABSTRACT

The last two decades have seen tremendous progress in the design and performance of mid-wavelength infrared (MWIR) type-II superlattices (T2SL) for detectors. The materials of focus have evolved from the InAs/(In)GaSb T2SL to include InAs/InAsSb T2SLs and most recently InGaAs/InAsSb SLs, with each materials system offering particular advantages and challenges. InAs/InAsSb SLs have the longest minority carrier lifetimes, and their best nBn dark current densities are <5X Rule '07 at high temperatures, while those of InAs/GaSb SLs and InGaAs/InAsSb SLs are <10X Rule '07. The quantum efficiency of all three SL detectors can still be improved, especially by increasing the diffusion length beyond the absorber length at low temperatures. Evidence of low temperature carrier localization is greatest for the two SLs containing ternary layers; however, the interface intermixing causing the localization is present in all three SLs. Localization likely does not affect the high temperature detector performance (>120 K) where these SL unipolar barrier detectors are diffusion-limited and Auger-limited. The SL barrier detectors remain diffusion-limited post proton irradiation, but the dark current density increases due to the minority carrier lifetime decreasing with increased displacement damage causing an increase in the trap density. For these SL detectors to operate in space, the continued understanding and mitigation of point defects is necessary.

Keywords: infrared, detector, superlattice, localization, radiation tolerance, MWIR, displacement damage

1. INTRODUCTION

Mid-wavelength infrared (MWIR) type-II superlattices (T2SLs) comprised of III-V materials have been of interest since the superlattice invention in 1970.[1] The last two decades, in particular, have seen tremendous progress in the design and performance of MWIR T2SLs for detectors. The materials of focus have evolved from the initial InAs/(In)GaSb T2SL [2] to include InAs/InAsSb T2SLs[3] and, most recently, InGaAs/InAsSb SLs,[4] with each materials system offering particular benefits and challenges, as shown in Table 1 below. As the material quality of the InAs/(In)GaSb SLs increased to the point of being viable for devices,[5] the problem of short minority carrier lifetimes limited by Shockley-Read-Hall (SRH) recombination was exposed.[6, 7] Then InAs/InAsSb SLs were found to have longer minority carrier lifetimes[8, 9] at the cost of lower absorption coefficients[10] due to the strain-balanced (on GaSb substrates) layer thicknesses requirement and smaller valence band offsets (VBO) than those of InAs/(In)GaSb SLs. To address the lower absorption coefficient of InAs/InAsSb SLs, InGaAs/InAsSb SLs have been designed with approximately equal layer thicknesses, leading to higher wave function overlaps and a demonstrated a 30-35% increase in the absorption coefficient as compared to the reference InAs/InAsSb SL design.[4] Another advantage of the InGaAs/InAsSb SLs is the potential for increased vertical minority carrier hole mobility as compared to the InAs/InAsSb SL due to less hole confinement leading to lower hole effective masses. However, recent calculations[11] have shown that for the ~5.5 μm MWIR T2SLs designs considered, the vertical minority carrier hole conductivity effective masses of the InAs/InAsSb and InAs/ GaSb SLs are approximately equal, explaining the reasonable InAs/InAsSb SL detector performance despite the expected high band edge hole masses.

*Elizabeth.Steenbergen.1@us.af.mil

Table 1. Benefits and challenges of InAs/GaSb, InAs/InAsSb, and InGaAs/InAsSb SLs.

	InAs/GaSb SL	InAs/InAsSb SL	InGaAs/InAsSb SL
Benefits	• Larger VBO • Higher absorption	• Long minority carrier lifetime, > 1 µs • MBE: 1 shutter/valve	• Higher absorption • Potential for higher hole mobility
Challenges	• Short minority carrier lifetime, < 100 ns • MBE: 4 shutters	• Lower absorption • Lower hole mobility • p-type passivation • Lack of hole blocking barriers	• $In_{0.80}Ga_{0.20}As/InAs_{0.65}Sb_{0.35}$ design limit for MWIR on GaSb • MBE: 2 shutters/1 valve

Figure 1 illustrates how the number of publications in the SL research field has grown over time: the InAs/GaSb SL dominates the research field to this day; InAs/InGaSb SL research was most significant in the 1990's, when we also see the InAs/InAsSb SL and InGaAs/InAsSb SL being examined to a lesser extent and primarily for laser applications. The first decade of this century saw great improvements in the InAs/GaSb SL detector performance (see the dark current density reduction shown in Figure 2), in large part due to barrier device architectures,[12-14] such that the technology limitation became the absorber minority carrier recombination lifetime.
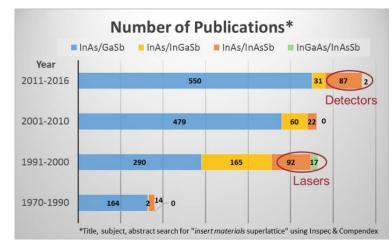

Figure 1. Number of publications reported from a title, subject, and abstract search using keywords "MaterialA MaterialB Superlattice" from 1970 to 2016. InAs/GaSb is shown in blue; InAs/InGaSb is shown in yellow; InAs/InAsSb is shown in orange; and InGaAs/InAsSb is show in green.

The revival of InAs/InAsSb SLs for detector applications seen in the last five years in Figure 1 resulted from the experimental demonstration of longer minority carrier lifetimes.[8, 9, 15] However, as shown in Figure 2, few publications exist in the literature on MWIR InAs/InAsSb SL detectors thus far. The InAs/InAsSb SL detectors using the PIN architecture from Prof. Krishna's group[16-18] exhibit higher dark currents than the W-structure nBn device from Sandia,[19] the MWIR portion of a dual band device from Prof. Razeghi's group,[20] and the nBn device from Raytheon and Sandia.[21] The single dark current data point for the InGaAs/InAsSb SL nBn[22] is very close to the best reported dark current for the InAs/InAsSb nBn at 77 K.

Although the latest MWIR detector dark current densities are similar for the three main SLs discussed here, the minority carrier lifetimes are quite different. Figure 3 displays minority carrier lifetimes reported in the literature at 77 K for several binary, ternary, and SL materials. However, keep in mind that the dominating carrier recombination mechanism is not listed in this plot, and it varies for the different materials and temperatures. The minority carrier lifetimes of InAs, InAsSb, and InSb reported before 2012 are approximately two to three times that of GaSb.[7] More recent InAsSb lifetimes have been reported to be an order of magnitude longer,[9, 23] while HgCdTe lifetimes are consistently an order of magnitude, or more, higher than the binaries. The InAs/GaSb SL minority carrier lifetimes are consistently less than the lifetime of GaSb, leading many to conclude that GaSb is the culprit causing the short SL carrier lifetime. The InAs/InAsSb SL lifetimes are slightly greater than the InAs lifetime and on the order of the latest InAsSb lifetime values.
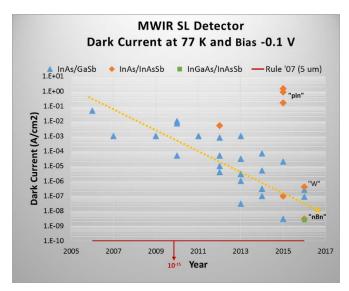
Figure 2. Approximate dark current densities for MWIR SL detectors operating near 77 K and -0.1 V reported in the literature from a title, subject, and abstract search using keywords "MaterialA MaterialB superlattice mid wave infrared detector dark current." InAs/GaSb is shown in blue triangles; InAs/InAsSb is shown in orange diamonds; InGaAs/InAsSb is show in green squares; and Rule '07 [24] is 10^{-15} A/cm² for a 77 K 5-μm bandgap detector. The dashed yellow line is a guide for the eye.

The limited InGaAs/InAsSb SL carrier lifetime data is similar to the InAs/GaSb SL, in part due to the doping levels being *n*-type mid-10^{16} cm^{-3}.[22] Also, the InAs/InAsSb SL lifetimes are comparable to some of the HgCdTe lifetimes. One reason for the InAs/InAsSb SL lifetime being longer than that of its constituents is carrier localization, which is discussed in Section 2. Detector performance and limitations of these SLs are discussed in Section 3, followed by radiation tolerance in Section 4. Outlooks and conclusions are given in Sections 5 and 6, respectively.
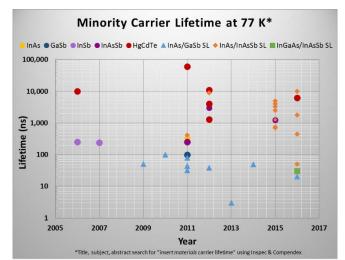

Figure 3. Survey of minority carrier lifetimes reported in the literature for InAs, GaSb, InSb, InAsSb, HgCdTe, InAs/GaSb SLs, InAs/InAsSb SLs, and InGaAs/InAsSb SLs.

2. CARRIER LOCALIZATION

Carrier localization is due to local spatial variations in the conduction and valence band potentials due to impurities, composition variation, or layer thickness variation for extremely thin layers, such as in SLs. These local potentials result in tail states at lower energies than the bandgap in the joint density of states; and thus, under low temperature these states can trap carriers, and under low injection conditions, these states can be observed. Two common manifestations of carrier localization are extremely long carrier lifetimes[23] and photoluminescence (PL) peak blue shifts at low temperatures.[25]

Devices operating at temperatures higher than the delocalization temperature may experience no deleterious effects from carrier localization, but detectors operating at temperatures less than ~80 K with low background doping and low incident light intensities may manifest symptoms of carrier localization, such as reduced carrier collection efficiency resulting in lower quantum efficiency. A discussion of carrier localization in the three types of SLs follows, with numerical comparisons visible in Table 2 below.

2.1 InAs/GaSb SL

Reports of the PL peak blue-shifting with increasing temperature have appeared in the literature for InAs/GaSb SLs, but the explanation was not attributed to carrier localization at the time. For instance, a short period (24 Å) InAs/GaSb SL exhibited an ~4 meV PL peak blue shift from 5 K to 80 K, and the low-energy side of the PL peak had a shallower slope than the high-energy side below 80 K,[26] indicating the presence of tail states in the joint density of states. The behavior of this sample is indicative of carrier localization. Other samples, however, exhibit a PL peak blue shift which is not conclusively due to carrier localization. For example, the 26 Å InAs/20 Å GaSb SL and 33 Å InAs/20 Å GaSb SLs have PL peak blue shifts below 80 K, 4 meV and 2 meV, respectively, but the shape of the low-energy side of the PL peak is sharp and does not obviously indicate tail states. The decreasing blue shift with increasing SL period is symptomatic of carrier localization; however, a transition involving a shallow dopant in the SL close to the bandgap[27] could also potentially account for this PL peak blue shift. A decreasing carrier lifetime from 11 K to 100 K is also a possible sign of carrier localization, but for an InAs/InGaSb SL, it was attributed to SRH-recombination.[28] Table 2 shows PL peak blue shifts ranging from 7 meV to 2 meV as the PL peak position wavelength increases from 2.1 µm to 7.2 µm for different InAs/GaSb SL designs.

Table 2. Summary of SL PL peak position and blue shift for InAs/GaSb, InAs/InAsSb, and InGaAs/InAsSb SLs.

SL Materials	PL Peak Location 77 K (meV, µm)	Excitation Intensity (W/cm^2)	PL peak blue shift (meV)
InAs/GaSb			
12 Å InAs/300 Å GaSb	584, 2.1	50	7 [29]
13 Å InAs/11 Å GaSb	325, 3.8	5	4 [26]
26 Å InAs/20 Å GaSb	223, 5.6	1.5	4
33 Å InAs/20 Å GaSb	172, 7.2	3	2
InAs/InAsSb			
52 Å InAs/47 Å InAs$_{0.81}$Sb$_{0.19}$	253, 4.9	0.05	3 [23]
67 Å InAs/18 Å InAs$_{0.66}$Sb$_{0.34}$	242, 5.1	1.5	8 [25]
52 Å InAs/17 Å InAs$_{0.65}$Sb$_{0.35}$	239, 5.2	4	7
67 Å InAs/18 Å InAs$_{0.64}$Sb$_{0.36}$	229, 5.4	1.5	8 [25]
68 Å InAs/18 Å InAs$_{0.61}$Sb$_{0.39}$	215, 5.8	1.5	8 [25]
82 Å InAs/25 Å InAs$_{0.65}$Sb$_{0.35}$	195, 6.4	0.8	8 [25]
73 Å InAs/22 Å InAs$_{0.65}$Sb$_{0.35}$	208, 6.0	1.5	2 [25]
InGaAs/InAs$_{0.65}$Sb$_{0.35}$			
26 Å In$_{0.80}$Ga$_{0.20}$As/27 Å InAs$_{0.65}$Sb$_{0.35}$	246, 5.0	4	14
40 Å In$_{0.95}$Ga$_{0.05}$As/20 Å InAs$_{0.65}$Sb$_{0.35}$	237, 5.2	4	12
33 Å In$_{0.90}$Ga$_{0.10}$As/23 Å InAs$_{0.65}$Sb$_{0.35}$	238, 5.2	4	9

2.2 InAs/InAsSb SL

Carrier localization in the InAs/InAsSb SLs was first suggested to explain the low temperature behavior of the minority carrier lifetime of shorter period MWIR samples.[15] The carrier lifetime for MWIR SLs decreased with increasing temperature until ~80 K after which it increased until ~200 K before decreasing again. At that time, the spectral PL data was taken under high excitation conditions and thus did not give a clear confirmation of localization. Later, low-excitation PL spectra[25] for the same samples exhibited peak blue shifts at low temperatures, non-monotonic full-width-half-maximums (FWHMs), and decreasing-increasing-decreasing integrated intensities as the temperature increased. This behavior identifies carrier localization and illustrates the importance of using low-excitation conditions to detect carrier localization. By comparing the carrier lifetime temperature-dependence and PL spectra of a bulk InAsSb sample lattice-matched to GaSb, a MWIR InAs/InAsSb SL, and a LWIR InAs/InAsSb SL, the MWIR SL 12.8 µs lifetime at 15 K was

determined to be due to carrier location due to its decrease with increasing temperature.[23] The physical cause of the carrier localization was found to be the InAs/InAsSb interface disorder.[23] Therefore, SLs with smaller periods may have greater effects from interface disorder and deeper localization potentials.[25] Table 2 shows the InAs/InAsSb SL PL peak blue shifts ranging from 2 meV to 8 meV, comparable to those of the InAs/GaSb SLs.

2.3 InGaAs/InAsSb SL

The PL peak positions and FWHMs vs. temperature are shown in Figure 4 below for a recent set of $In_{1-y}Ga_yAs/InAs_{0.65}Sb_{0.35}$ SLs,[4] whose growth conditions were not optimized. The PL peak positions blue shifts and the FWHM peaks near 40 K are evidence of carrier localization. It is reasonable to expect some interface disorder between the two ternary SL layers leading to carrier localization due to the growth not being optimized. As seen in Table 2, the peak position blue shift ranges from 5 meV to 14 meV for these InGaAs/InAsSb SLs, which is approximately 3-6 meV greater than that of the other two SLs above. With further growth optimization, it may be possible to lower the blue shift, but the interface between two ternary materials is inherently complicated.
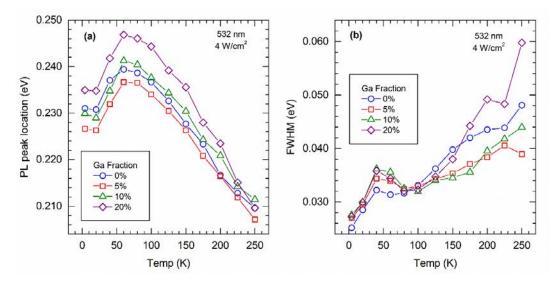

Figure 4. PL peak location (a) and FWHM (b) vs. temperature for a set of $In_{1-y}Ga_yAs/InAs_{0.65}Sb_{0.35}$ superlattices. The peak locations shows a blue shift for temperatures less than 60 K while the FHWMs are non-monotonic with a peak near 40 K – both characteristic of carrier localization.

Interface atomic intermixing or disorder is evident in both the InAs/GaSb SLs[30-32] and the InAs/InAsSb SLs,[33, 34] and therefore, is expected to be found in the InGaAs/InAsSb SLs as well. It is debatable whether this SL interface disorder can be reduced by optimizing growth conditions or whether it is a fundamental property of these materials. If it is a basic characteristic of these material systems, effects of such disorder, including carrier localization potentially lowering detector collection efficiency, must be taken into account when choosing the material for a specific infrared device application. If the interface intermixing in these SLs can be reduced by engineering growth optimization, the effects of achieving the designed abrupt interfaces on SL device performance will be greatly anticipated.

3. DEVICE PERFORMANCE

Infrared detector performance is governed by several metrics: cutoff wavelength, dark current density, external quantum efficiency (EQE), and noise factors, from which the responsivity and detectivity can be calculated. The metric requirements differ depending on the application. Currently, the dark current density of SL infrared detectors is commonly compared to Rule '07 [24] to gauge the detector quality. Rule '07 is the 2007 (updated in 2010[24] and still holds today) empirical expression describing the compiled dark current densities of the best diffusion-limited, planar, *pn* HgCdTe MWIR-LWIR detectors operating at T >77 K and fabricated at Teledyne Imaging Sensors. This is a reasonable comparison to make, provided that the assumptions for which the rule is valid are met for the SL detectors, since SL detectors may theoretically outperform HgCdTe when Auger recombination is properly band-engineered[35] and is the limiting recombination mechanism. One obvious difference between the SL detectors and the HgCdTe detectors used for Rule '07

is the device architecture: SL detectors are typically vertical *pin* or barrier-containing (*nBn*, *pBn*, CBIRD, etc…) structures, while the HgCdTe detectors were planar *pn* structures. Another difference is the high EQE (60-80%)[24] of HgCdTe as compared to the lower EQE (~30-48%)[5, 36-39] of InAs/GaSb SL detectors. A low EQE results in lower responsivity and thus lower detectivity, which may make the SL detector unsuitable for its application regardless if it has a dark current density below that of Rule '07. However, as seen in Figure 2, the 77 K MWIR SL detector dark currents are six orders of magnitude higher than Rule '07. Finally, the dark current densities of the HgCdTe detectors comprising the Rule '07 data set were limited by the Auger-1 process, but InAs/InAsSb SL detectors tend to be limited by SRH or Radiative recombination at low temperatures and Auger recombination at higher temperatures.[40-42] Therefore, Rule '07 is a good comparison metric for SL and HgCdTe infrared detectors when the SL EQE is 60-80%, the dark current is diffusion-limited, and the carrier lifetime is Auger-limited.

As one of the appeals of SL detectors is the suitability for high operating temperature (HOT) detector applications, it is worthwhile to examine the dark current performance of the three types of SL detectors at high temperatures, defined as 120-150 K and above, where Auger recombination tends to dominate. Similarly to the 77 K trend depicted in Figure 2, the dark current of SL-based barrier detectors at high temperatures is rapidly approaching Rule '07, mainly due to improved SL growth quality leading to long minority carrier lifetimes and low background doping levels. Chen *et al*. have reported an InAs/GaSb SL *pπMn* gated detector with a 4.8 µm cutoff, peak EQE of 52%, and dark current nearing 10X Rule '07 at 150 K.[36] The most recent work reported by Rhiger *et al*. and Kadlec *et al*. reveal MWIR InAs/InAsSb *nBn* detectors with dark current densities as low as 5X Rule '07 at 150 K.[21, 42] Similarly, the dark current reported for the InGaAs/InAsSb SL *nBn* detectors is also within 10X Rule '07 at temperatures above 140 K where the EQE is ~25%.[22] Since the variation in the HgCdTe data is 0.4-2.3X Rule '07, SL dark current densities within 5-10X Rule '07 are very promising for high temperature operation provided that the EQE is also sufficient. One thing common to all of these SL detectors is that they use the barrier architectures and exhibit diffusion-limited performance at high temperatures. This implies the necessity of using the *nBn* architecture with these SL materials to suppress generation-recombination (GR) and surface leakage currents as SRH trap states and surface passivation are still materials problems.

Surface passivation is key to suppress sidewall leakage currents that are more apparent for focal plane array (FPA) pixel dimensions, ~20-40 µm, when the pixels are fully reticulated. Several techniques have been applied to InAs/GaSb SL detectors with varying results: overgrowth with larger bandgap materials (ZnTe), chalcogenides (ZnS), encapsulation with SiO_2, Si_3N_4, Al_2O_3,[38] SU-8 photoresist,[43] or polyimides, and sidewall gating.[36] The SU-8 photoresist passivation resulted in decreasing the dark current density by four orders of magnitude; however, it was still orders of magnitude higher than Rule '07 at 77 K with a EQE of 33%. Sidewall gating also reduced the dark current density by several orders of magnitude, but the required gate voltage needs to be reduced. Minimal reports of bulk[44] or surface passivation[17] have been published for InAs/InAsSb SLs and none were found for InGaAs/InAsSb SLs. Therefore passivation work remains for these SLs.

The EQE of MWIR InAs/GaSb SL detectors has doubled over the past decade from near 25% to ~50% [5, 36, 38] with improved detector design. A MWIR InAs/InAsSb SL detector has been reported with an EQE of 45% at 77 K [20], and the EQE of the InGaAs/InAsSb SLs is ~25% at 160 K.[22] Additionally, the EQE of many of these detectors increases with increasing temperature.[5, 22, 37, 45, 46] Since these EQE values are reported for a wavelength considerably shorter than the bandgap, it is unlikely that carrier localization, which occurs below the band edge, is the sole cause for this increase in the EQE with temperature. The change in the SL bandgap with temperature is not great enough to cause some of the considerable increases in EQE (~3X) [37] that have been reported. Rather, the minority carrier diffusion length, $L_D = (\mu\tau\, kT/q)^{1/2}$, being smaller than the absorber length at lower temperatures, possibly due to carrier localization, results in less than unity carrier collection efficiency; thus decreasing the external EQE. The temperature dependence of the diffusion length is complicated: the mobility, μ, and lifetime, τ, temperature dependences vary based on the dominating scattering and recombination mechanisms in a specific temperature regime. A minority carrier hole diffusion length of 750 nm at 6 K was reported for an InAs/InAsSb nBn detector with a 2.4 µm thick absorber[47] and of 100 nm at 77 K for a set of InAs/GaSb SL with 0.5 µm, 1.0 µm, and 4.0 µm thick absorbers,[48] confirming the short diffusion length at low temperature. The EQE decreasing with decreasing temperature poses a problem if the detector is cooled to achieve lower dark current to meet performance specifications for low background applications, such as astronomy and space missions.

4.   RADIATION TOLERANCE

Infrared detectors used in space-based imaging systems must be able to withstand and perform well within the radiation environment. Proton radiation is of particular interest as it occurs in the Van Allen radiation belt and due to solar particle

events. Protons can cause displacement damage, resulting in additional point defects, when their incoming energy causes an atom to be removed from its lattice site. These additional defects are detrimental to the detector performance, and their effects must be characterized before the detector can be deemed suitable for space applications. Additionally, space applications have very low backgrounds which require low detector operating temperatures. The goal of SL unipolar barrier detector dark current density being less than or equivalent to Rule '07 at 130 K with high EQE has yet to be realized.

A recent study of an InAs/InAsSb SL at room temperature during 63-MeV proton irradiation found the carrier lifetime decreased to approximately half of its pre-radiation value and the trap density increased ~5X after a total fluence of 7.5×10^{11} protons/cm^2/s (ionizing dose of 100 kRad(Si)).[49] These results are a best case scenario as some displacement damage anneals out above typical detector operating temperatures (~80-120 K).[50] Therefore, more realistic performance results are found when keeping the detector at its operating temperature during the proton irradiation, and then raising the temperature in a controlled manner to investigate the effects of annealing.[50-52] Minority carrier lifetime measurements carried out in this way on nine III-V SL samples found the carrier lifetime decreased between 45% and 94% after a total fluence of 7.5×10^{11} protons/cm^2/s (ionizing dose of 100 kRad(Si)), with most samples showing a considerable increase in lifetime, although not back to pre-radiation values, after a room temperature anneal.[52] A convenient way to compare detector materials is to determine the rate of minority carrier lifetime degradation vs. proton fluence, or the slope of the recombination rate vs. proton fluence as shown below in Figure 5. This figure compares a III-V alloy sample (black curve), an InAs/InAsSb SL sample (red curve), and a HgCdTe sample (green curve), and it makes it clear that the III-V SLs are less radiation hard than HgCdTe of similar cutoff wavelengths.[52]
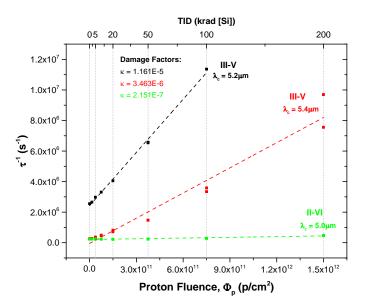

Figure 5. Reciprocal lifetime vs. proton fluence for two III-V samples (black curve is an alloy, red curve is an InAs/InAsSb SL) and one II-VI sample (green curve is HgCdTe). The slope determines the damage factors, as shown in the inset.

The MWIR InAs/GaSb SL detector of a dual-band pBp detector had an order of magnitude higher dark current density and ~10% lower EQE after proton irradiation of 7.5×10^{11} protons/cm^2/s (ionizing dose of 100 kRad(Si)).[50] After a room temperature anneal, the dark current density reduced to 50% of its post-radiation value, and the EQE recovered to within 5% of its pre-radiation value. Dark current density damage factors for several InAs/InAsSb SL nBn detectors were compiled and plotted against $1/(\lambda_c T)$, similarly to Rule '07.[51] This plot indicated that the dark current density increased due to a decrease in minority carrier lifetime with increased displacement damage due to proton irradiation and that the dark current density remained diffusion limited as desired for the ideal nBn architecture. The characterization of a III-V nBn FPA under proton irradiation of 7.5×10^{11} protons/cm^2/s (ionizing dose of 100 kRad(Si)) concluded that the dark current density increased 1.6X and the quantum efficiency decreased 10% from a median value of 63%.[53] To increase the performance of these SL nBn detectors for space applications, the initial carrier lifetime must be high, and thus the trap density and background doping low, the dark current low, and the quantum efficiency high. As displacement damage due to proton radiation induces additional defect trap states, a continued understanding and mitigation of point defects and SRH states in these SLs is needed.

5. OUTLOOK

Significant progress has been made in MWIR SL detectors in the past two decades with new architectures greatly lowering the dark current densities and new materials increasing the minority carrier lifetimes. However, the quantum efficiency remains lower than desired and required for many strategic applications. Efforts to increase the MWIR detector quantum efficiency have involved increasing the cutoff wavelength, absorption coefficient, minority carrier diffusion length. To increase the band edge absorption coefficient and extend the cutoff wavelength, there is a trend toward using ternary bulk absorbers with extended cutoff wavelengths on different lattice constants than the typical substrates. A MWIR nBn detector based on the AlSb lattice constant and using an $InAs_{0.81}Sb_{0.19}$ absorber had a 150 K λ_c = 5.3 µm, a dark current density within 5X Rule '07, and a EQE of 44% (42% at 77 K) at 3.4 µm.[54] Incorporating an InSb monolayer after every 14 monolayers of $InAs_{0.92}Sb_{0.08}$ for the absorber for an nBn detector on GaSb resulted in extending the cutoff wavelength to 4.8 µm at 160 K, a dark current density within 10X of Rule '07, and a double-pass EQE of ~50% at ~3.5 µm that did not change with temperature.[55] These ternary absorbers also displayed GR and tunneling currents at lower temperatures. Therefore, for applications that require lower operating temperatures, the defect problems in III-V absorber materials, SLs and bulk, will have to be solved.

6. CONCLUSION

MWIR InAs/GaSb, InAs/InAsSb and InGaAs/InAsSb SLs have their similarities and differences. They all have the design flexibility to engineer the bandgap and Auger recombination coefficient. Where the InAs/GaSb SL and InGaAs/InAsSb SL have higher absorption coefficients than the InAs/InAsSb SL, the InAs/InAsSb SL has longer minority carrier lifetimes and less complicated MBE growth. Low temperature carrier localization is clearly evident in the InAs/InAsSb SL and the InGaAs/InAsSb SL but less so in the InAs/GaSb SL, perhaps due to its longer development at this point. With the addition of barrier architectures in these SL detectors, all three SL type detectors have dark current densities approaching that of Rule '07 (5-10X) at high temperatures (120-150 K). However, the detector EQE remains lower than desired and passivation remains to be perfected. To be able to withstand proton radiation for space-based imaging applications, the initial detector minority carrier lifetime and diffusion length need to be long while the background carrier and trap densities need to be small. The performance of MWIR SL detectors has increased significantly in the last two decades, but native defects continue to plague even the highest quality SL materials.

REFERENCES

[1] Esaki, L. and Tsu, R., "Superlattice and negative differential conductivity in seminconductors," IBM J. Res. Dev., 1970.

[2] Sai-Halasz, G. A., Tsu, R., and Esaki, L., "A new semiconductor superlattice," Appl. Phys. Lett. 30(12), 651 (1977).

[3] Zhang, Y.-H., "Antimonide-related strained-layer heterostructures," [Optoelectronic Properties of Semiconductors and Superlattices], Gordon, Breach, 461-500 (1997).

[4] Ariyawansa, G., Reyner, C. J., Steenbergen, E. H., Duran, J. M., Reding, J. D., Scheihing, J. E., Bourassa, H. R., Liang, B. L., and Huffaker, D. L., "InGaAs/InAsSb strained layer superlattices for mid-wave infrared detectors," Appl. Phys. Lett. 108(2), 022106 (2016).

[5] Wei, Y., Hood, A., Yau, H., Gin, A., and Razeghi, M. "Uncooled operation of type-II InAs/GaSb superlattice photodiodes in the midwavelength infrared range," Appl. Phys. Lett. 86, 233106 (2005).

[6] Donetsky, D., Svensson, S., Vorobjev, L. and Belenky, G. "Carrier lifetime measurements in short-period InAs/GaSb strained-layer superlattice structures," Appl. Phys. Lett. 95, 212104 (2009).

[7] Svensson, S. P., Donetsky, D., Wang, D., Hier, H., Crowne, F. J. and Belenky, G., "Growth of type II strained layer superlattice, bulk InAs and GaSb materials for minority lifetime characterization," J. Cryst. Growth 334, 103-107 (2011).

[8] Steenbergen, E. H., Connelly, B. C., Metlcalfe, G. D., Shen, H., Wraback, M., Lubyshev, D., Qiu, Y., Fastenau, J. M., Liu, A. W. K., Elhamri, S., Cellek, O. O. and Zhang, Y.-H., "Significantly improved minority carrier lifetime observed in a long-wavelength infrared III-V type-II superlattice comprised of InAs/InAsSb," Appl. Phys. Lett. 99, 251110 (2011).

[9]   Olson, B. V., Shaner, E. A., Kim, J. K., Klem, J. F., Hawkins, S. D., Murray, L. M., Prineas, J. P., Flatte, M. E. and Boggess, T. F., "Time-resolved optical measurements of minority carrier recombination in a mid-wave infrared InAsSb alloy and InAs/InAsSb superlattice," Appl. Phys. Lett. 101, 092109 (2012).

[10] Klipstein, P. C., Livneh, Y., Glozman, A., Grossman, S., Klin, O., Snapi N., and Weiss, E., "Modeling InAs/GaSb and InAs/InAsSb Superlattice Infrared Detectors," J. Electron. Mater. 43(8), 2984-2990 (2014).

[11] Ting, D. Z., Soibel, A. and Gunapala, S. D., "Hole effective masses and subband splitting in type-II superlattice infrared detectors," Appl. Phys. Lett. 108(18), 183504 (2016).

[12] Maimon, S. and Wicks, G. W., "nBn detector, an infrared detector with reduced dark current and higher operating temperature," Appl. Phys. Lett. 89(15), 151109 (2006).

[13] Ting, D. Z.-Y., Soibel, A., Hill, C. J., Nguyen, J., Keo, S. A., Rafol, S. B., Yang, B., Lee, M. C., Mumolo, J. M., Liu, J. K., Hoglund, L., and Gunapala, S. D., "Antimonide superlattice complementary barrier infrared detector (CBIRD)," Infrared Phys. & Techn. 54(3), 267-272 (2011).

[14] Klipstein, P., ""XBn" barrier photodetectors for high sensitivity and high operating temperature infrared sensors," Proc. SPIE 6940, 69402U (2008).

[15] Steenbergen, E. H., Connelly, B. C., Metcalfe, G. D., Shen, H., Wraback, M., Lubyshev, D., Qiu, Y., Fastenau, J. M., Liu, A. W. K., Elhamri, S., Cellek, O. O., and Zhang, Y.-H., "Temperature-dependent minority carrier lifetimes of InAs/InAsSb type-II superlattices," Proc. SPIE 8512, 85120L (2012).

[16] Schuler-Sandy, T., Myers, S., Klein, B., Gautam, N., Ahirwar, P., Tian, Z.-B., Rotter, T., Balakrishnan, G., Plis, E. and Krishna, S., "Gallium free type II InAs/InAsSb superlattice photodetectors," Appl. Phys. Lett. 101, 071111 (2012).

[17] Plis, E. A., Schuler-Sandy, T., Ramirez, D. A., Myers, S. and Krishna, S., "Dark current reduction in InAs/InAsSb superlattice mid-wave infrared detectors through restoration etch," Electron. Lett. 51(24), 2009-2010 (2015).

[18] Schuler-Sandy, T., Klein, B., Casias, L., Mathews, S., Kadlec, C., Tian, Z., Plis, E., Myers, S., and Krishna, S., "Growth of InAs-InAsSb SLS through the use of digital alloys," J. Cryst. Growth 425, 29-32 (2015).

[19] Olson, B. V., Kim, J. K., Kadlec, E. A., Klem, J. F., Hawkins, S. D., Coon, W. T., Fortune, T. R., Tauke-Pedretti, A., Cavaliere, M. A. and Shaner, E. A., "Optical and electrical properties of narrow-bandgap infrared W-structures superlattices incorporating AlAs/AlSb/AlAs barrier layers," Appl. Phys. Lett. 108, 25210 (2016).

[20] Haddadi, A., Chevallier, R., Chen, G., Hoang, A. M. and Razeghi, M., "Bias-selectable dual-band mid-/long-wavelength infrared photodetectors based on InAs/InAsSb type-II superlattices," Appl. Phys. Lett. 106, 011104 (2015).

[21] Rhiger, D. R., Smith, E. P., Kolasa, B. P., Kim, J. K., Klem, J. F. and Hawkins, S. D., "Analysis of III-V Superlattice nBn Device Characteristics," J. Electron. Mater. 45(9), 4646-4653 (2016).

[22] Ariyawansa, G., Reyner, C. J., Duran, J. M., Reding, J. D., Scheihing, J. E. and Steenbergen, E. h., "Unipolar infrared detectors based on InGaAs/InAsSb ternary superlattices," Appl. Phys. Lett. 109, 021112 (2016).

[23] Lin, Z.-Y., Liu, S., Steenbergen, E. H. and Zhang, Y.-H., "Influence of carrier localiztion on minority carrier lifetime in InAs/InAsSb type-II superlattices," Appl. Phys. Lett. 107, 201107 (2015).

[24] Tennant, W., ""Rule 07" Revisited: Still a Good Heuristic Predictor of p/n HgCdTe Photodiode Performance," J. Electron. Mater. 39(7), 1030 (2010).

[25] Steenbergen, E. H., Massengale, J. A., Ariyawansa, G. and Zhang, Y.-H., "Evidence of carrier localization in photoluminescence spectroscopy studies of mid-wavelength infrared InAs/InAsSb type-II superlattices," J. Lumin. 178, 451-456 (2016).

[26] Haugan, H. J., Szmulowicz, F., Brown, G. J., Ullrich, B., Munshi, S. R., Wickett, J. C. and Stokes, D. W., "Short-period InAs/GaSb superlattices for mid-infrared photodetectors," phys. stat. sol. (c). 4(5), 1702-1706 (2007).

[27] Flatte, M. E. and Pryor, C. E., "Defect states in type-II strained-layer superlattices," Proc. SPIE 7608, 760824 (2010).

[28] Connelly, B. C., Metcalfe, G. D., Shen, H. and Wraback, M., "Time-Resolved Photoluminescence Study of Carrier Recombination and Transport in Type-II Superlattice Infrared Detector Materials," Proc. SPIE 8704, 87040V (2013).

[29] Bertru, N., Baranov, A. N., Cuminal, Y., Boissier, G., Alibert, C., Joullie, A. and Lambert, B., "Spontaneous emission from InAs/GaSb quantum wells grown by molecular beam epitaxy," J. Appl. Phys. 85(3), 1989-1991 (1999).

[30] Steinshnider, J., Harper, J., Weimer, J., Lin, C.-H., Pei, S. S. and Chow, D. H., "Origin of Antimony Segregation in GaInSb/InAs Strained-Layer Superlattices," Phys. Rev. Lett. 85(21), 4562 (2000).

[31] Ashuach, Y., Kauffmann, Y., Isheim, D., Amouyal, Y., Seidman, D. and Zolotoyabko, E.,"Atomic intermixing in short-period InAs/GaSb superlattices," Appl. Phys. Lett. 100, 241604 (2012).

[32] Mahalingam, K., Haugan, H. J., Brown, G. J., Eyink, K. G. and Jiang, B. "Quantitative strain analysis of interfaces in InAs/GaSb superlattices by aberration-corrected HAADF-STEM," Proc. SPIE 8268, 826831 (2012).

[33] Ouyang, L., Steenbergen, E. H., Zhang, Y.-H., Nunna, K., Huffaker, D. L. and D. J. Smith, "Structural properties of InAs/InAs1–xSbx type-II superlattices grown by molecular beam epitaxy," J. Vac. Sci. Technol. B 30(2), 02B106-1-5, (2012).

[34] Shen, X.-M., Li, H., Liu, S., Smith, D. J. and Zhang, Y.-H., "Study of InAs/InAsSb type-II superlattices using high-resolution x-ray diffraction and cross-sectional electron microscopy," J. Crys. Growth 381, 1-5 (2013).

[35] Grein, C. H., Garland, J. and Flatte, M. E., "Strained and Unstrained Layer Superlattices for Infrared Detection," J. Electron. Mater. 38(8), 1800 (2009).

[36] Chen, G., Nguyen, B.-M., Hoang, A. M., Huang, E. K., Darvish, S. R. and Razeghi, M., "Elimination of surface leakage in gate controlled type-II InAs/GaSb mid-infrared photodetectors," Appl. Phys. Lett. 99(18), 183503 (2011).

[37] Asplund, C., von Wurtemberg, R. M., Lantz, D., Malm, H., Martijn, H., Plis, E., Gautam, N. and Krishna, S., "Performance of mid-wave T2SL detectors with heterojunction barriers," Infrared Phys. & Techn. 59, 22-27 (2013).

[38] Salihoglu, O., Muti, A., Kutluer, K., Tansel, T., Turan, R., Kocabas, C. and Aydinli, A., "Atomic layer deposited Al$_2$O$_3$ passivation of type II InAs/GaSb superlattice photodetectors," J. Appl. Phys. 111(7), 074509 (2012).

[39] Martyniuk, P. and Rogalski, A., "MWIR barrier detectors versus HgCdTe photodiodes," Infrared Phys. & Techn. 70, 125-128 (2015).

[40] Aytac, Y., Olson, B. V., Kim, J. K., Shaner, E. A., Hawkins, S. D., Klem, J. F., Flatte, M. E. and Boggess, T. F., "Temperature-dependent optical measurements of the dominant recombination mechinisms in InAs/InAsSb type-2 superlattices," Appl. Phys. Lett. 118, 125701 (2015).

[41] Hoglund, L., Ting, D. Z., Khoshakhlagh, A., Soibel, A., Hill, C. J., Fisher, A., Keo, S. and Gunapala, S. D., "Influence of radiative and non-radiative recombination on the minority carrier lifetime in midwave infrared InAs/InAsSb superlattices," Appl. Phys. Lett. 103, 221908 (2013).

[42] Kadlec, E. A., Olson, B. V., Goldflam, M. D., Kim, J. K., Klem, J. F., Hawkins, S. D., Coon, W. R., Cavaliere, M. A., Tauke-Pedretti, A., Fortune, T. R., Harris, C. and Shaner, E. A., "Effects of electron doping level on minority carrier lifetimes in n-type mid-wave infrared InAs/InAsSb type-II superlattices," Appl. Phys. Lett. 109(26), (2016).

[43] Kim, H. S., Plis, E., Myers, S., Khoshakhlagh, A., Gautam, N., Kutty, M. N., Sharma, Y. D., Dawson, L. R. and Krishna, S., "Improved performance of InAs/GaSb strained layer superlattice detectors with SU-8 passivation," Proc. SPIE 7467, 74670U (2009).

[44] Hossain, K., Hoglund, L., Phinney, L. C., Golding, T. D., Wicks, G., Khoshakhlagh, A., Ting, D.-Y., Soibel, A. and Gunapala, S. D., "Hydrogenation Defect Passivation for improved minority carrier lifetime in mid wavelength Ga-free InAs/InAsSb superlattices," J. Electron. Mater. 45(11), 5626-9 (2016).

[45] Zhu, Z. M., Bhattacharya, P., Plis, E., Su, X. H. and Krishna, S., "Low dark current InAs/GaSb type-II superlattice infrared photodetectrs with resonant tunnelling filters," J. Phys. D: Appli. Phys. 39, 4997-5001 (2006).

[46] Khoshakhlagh, A., Rodriguez, J. B., Plis, E., Bishop, G. D., Sharma, Y., Kim, H. S., Dawson, L. R. and Krishna, S., "Bias dependent dual band response from InAs/Ga(In)Sb type II strain layer superlattice detectors," Appl. Phys. Lett. 91, 263504 (2007).

[47] Zou, D., Liu, R., Wasserman, D., Mabon, J., He, Z.-Y., Liu, S., Zhang, Y.-H., Kadlec, E. A., Olson, B. V. and Shaner, E. A., "Direct minority carrier transport characterization of InAs/InAsSb superlattice nBn photodetectors," Appl. Phys. Lett. 106, 071107 (2015).

[48] Giard, E., Ribet-Mohamed, I., Jaeck, J., Viale, T., Haidar, R., Taalat, R., Delmas, M., Rodriguez, J.-B., Steveler, E., Bardou, N., Boulard, F. and Christol, P., "Quantum efficiency investigations of type-II InAs/GaSb midwave infrared superlattice photodetectors," J. Appl. Phys. 116, 043101 (2014).

[49] Hoglund, L., Ting, D. Z., Khoshakhlagh, A., Soibel, A., Fisher, A., Hill, C. J., Keo, S., Rafol, S. and Gunapala, S. D., "Influence of proton radiation on the minority carrier lifetime in midwave infrared InAs/InAsSb superlattices," Appl. Phys. Lett. 108, 263504 (2016).

[50] Cowan, V. M., Morath, C. P., Myers, S., Plis, E. and Krishna, S., "Radiation Tolerance of a Dual-Band IR Detector based on a pBp Architecture," Proc. SPIE 8353, 83530F (2012).

[51] Morath, C. P., Cowan, V. M., Treider, L. A., Jenkins, G. D. and Hubbs, J. E., "Proton irradiation effects on the performance of III-V-based unipolar barrier infrared detectors," IEEE T. Nucl. Sci. 62(2), 512-519 (2015).

[52] Jenkins, G. D., Morath, C. P. and Cowan, V. M., "Empirical trends of minority carrier recombination lifetime vs proton radiation for rad-hard IR detector materials," Proc. SPIE 9616, 96160G (2015).

[53] Hubbs, J. E., "Proton Radiation Experimental Results on an III-V nBn Mid-Wavelength Infrared Focal Plane Array," Proc. SPIE 9933, 993307 (2016).

[54] Baril, N., Brown, A., Maloney, P., Tidrow, M., Lubyshev, D., Qui, Y., Fastenau, J. M., Liu, A. W. K. and Bandara, S., "Bulk InAsxSb1-x nBn photodetectors with greater than 5 um cutoff on GaSb," Appl. Phys. Lett. 109, 122104 (2016).

[55] Soibel, A., Ting, D. Z., Hill, C. J., Fisher, A. M., Hoglund, L., Keo, S. A. and Gunapala, S. D., "Mid-wavelength infrared InAsSb/InSb nBn detector with extended cutoff wavelength," Appl. Phys. Lett. 109, 103505 (2016).